Monthly Weather Review

VOLUME 98, NUMBER 5

MAY 1970

UDC 551.577.21:551.501.81(084.3)(714) "1964-322"

PATTERN ANALYSIS OF ONE SUMMER'S MULTILEVEL MAPS OF MONTREAL RAIN

J. S. MARSHALL

McGill University, Montreal, Quebec

C. D. HOLTZ

Canadian Meteorological Service, Toronto, Ontario

ABSTRACT

For the summer of 1964, precipitation intensity in the vicinity of Montreal, observed by CPS-9 radar, was recorded on constant-altitude maps at six heights. To allow for attenuation (at $\lambda = 3.2$ cm) and other radar uncertainties, the distribution with rainfall rate R at 5,000 ft was matched to that for one rain gage at the surface. The extent (area $\times$ time) in excess of a given R decreased rapidly with increasing R and with increasing height: a factor 1000 from 0.4 to 100 mm hr^{-1}, a factor 10 per 15,000 ft. The pattern in plan at any height (with resolution limited to about 2 mi in the recorded maps) can be described in terms of cells with intensity decreasing outward approximately exponentially. A logarithmic function of intensity was used: $T = 1.66 \log (R/R_0)$ where $R_0 = 0.25$ mm hr^{-1}. The value of T for a contour bounding a central area A is given by $T = T_c - x$ where T_c is the maximum and $x = (A/17.5 \text{ n.mi.}^2)^{1/2}$. (With this relation, one can estimate peak intensity from the area bounded by any given intensity.) The number of cells having T_c greater than a given value of T, per 10^8 n.mi.^{2} of map area (as for hourly maps of area 20,000 n.mi.^{2} throughout a 5,000-hr summer) is N_0, where $\log N_0 = 8.8 - T - H$ and H = height/15,000 ft. As to shape, the maximum and minimum extents were always within a factor 6 of each other. Usually, the area in the horizontal section of a cell decreased with height. Occasionally it increased to a maximum, at about 20,000 ft, as much as four times greater than the area at 5,000 ft. These maxima aloft were generally identifiable with storms reaching 40,000 ft, which is tall for Montreal.

1. INTRODUCTION

In 1965, the nature of weather observed by airborne weather radar was studied at the instigation of the Air Transport Association. There was an obvious need to know, particularly for summer months, the amount of precipitation, in time and three-dimensional space, and the distribution of showers or storms with size and intensity. These data were available for the Montreal climate in the records of the McGill Weather Radar. Most of the work reported here was done at that time and presented in a scientific report of limited distribution (Marshall et al. 1965). The work has recently been revised and extended, and is reported here without the earlier specialized reference to airline operations. The data came from one rain-gage station and one CPS-9 radar, the former being introduced to mitigate statistically the distortion by attenuation of the latter. There is need for new radar observations of the sort described here, but with attenuation avoided by use of a longer wavelength than the 3.2 cm of the CPS-9. These would permit the present report to be superseded by something more reliable. There is also need for the extension of this sort of work to a wide range of climates. Some helpful studies in this general area, usually more specialized, have appeared since the first report, by Kessler (1966) for example. Our report has been put to use in more than one area of application (Altman 1968, Rogers and Rao 1968).

2. RAIN-GAGE AND RADAR INTERCOMPARISON

A digest of data for 5 summer months (May to September, 3,672 hr), from McGill Observatory gages, appears in figure 1. Total duration of recorded rain, at rates down to 0.1 mm hr^{-1}, was 208 hr. Standard tipping-bucket gages were used; but for the highest intensities, refined techniques were used for measuring times between tips (Weiss 1964).

In figure 1, the "McGill thresholds" marked on the logarithmic scale of rainfall rate with uniform spacing have their origin in weather radar studies. A suitable weather radar map indicates at every point the radar reflectivity of the rain, averaged over a considerable volume, the "contributing region," usually several thousand feet above the earth's surface. This reflectivity is related to the rate of rainfall at the same height, and

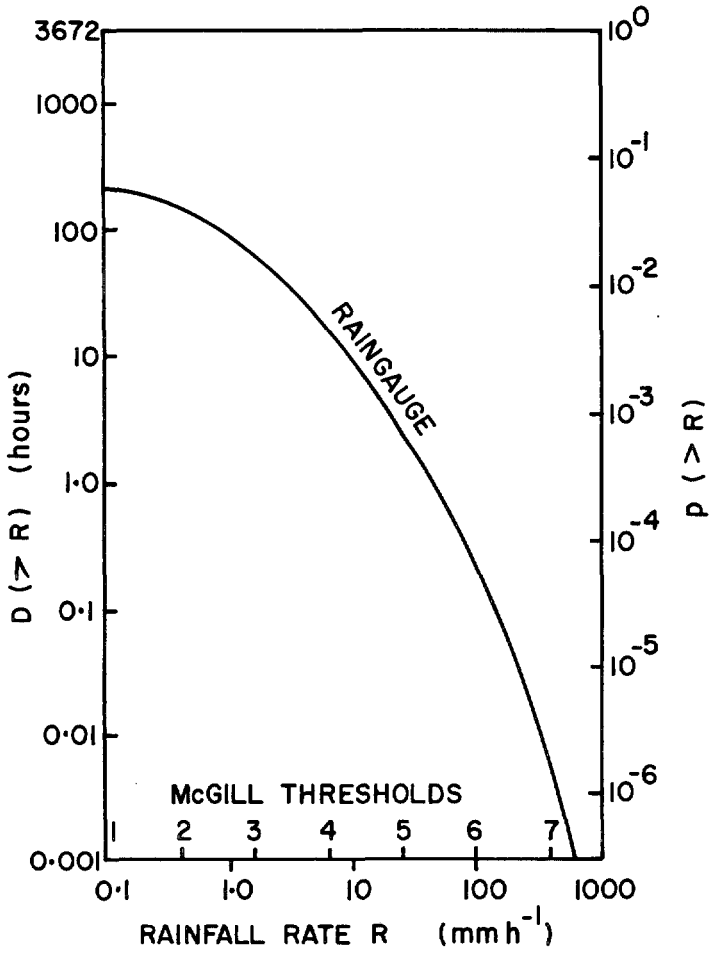

FIGURE 1.—Duration (left) and probability (right) of rain with intensity in excess of that given by the abscissa (in rate or "threshold"$=1.66 \log (R/R_0)$), for one summer season at Montreal.

so somewhat hopefully to the rate of rainfall at the surface. The relationship between the reflectivity quantity Z and the rate of rainfall R was first given by Marshall et al. (1947) as $Z=220\ R^{1.60}$, the coefficient being reduced later to 200. Many studies of the relationship have been made, notably by the Illinois State Water Survey (Stout and Mueller 1968, Cataneo 1969). The situation has been reviewed by Kessler and Wilk (1968).

In the stepped gray-scale maps in use at McGill since 1960, the shade of gray changes discontinuously at selected threshold values of Z and so of R, with a uniform shade n extending from threshold n to threshold $n+1$. In choosing threshold values, it was noted that, on the basis of $Z \propto R^{1.60}$, a factor 10 in Z (and so a term of 10 dB (decibels) in signal level) corresponded within a few parts percent to a factor 4 in rainfall rate R. A set of values of R was chosen, proceeding by uniform factors 4 from 0.10 mm hr^{-1} (the most sensitive threshold that it was hoped to maintain to range 100 mi with a CPS–9 radar) to 400 mm hr^{-1}, with an approximation in midscale to maintain round numbers: 0.10, 0.40, 1.6, 6.4, 25, 100, and 400 mm hr^{-1}. It is for $Z \propto R^{1.66}$ that factor 4 in Z would correspond to 10 dB in Z-level; for $Z \propto R^{1.60}$, the exact correspondence is to 9.63 dB, and the discrepancy can be awkward.

This series of threshold values that had been built into the radar records was found very convenient in the present work, within which much reference is made to them. Without recommending their perpetuation as an additional scale of precipitation intensity, we shall refer to them as "McGill-1960 thresholds." Alongside this discontinuous usage, it is compatible and helpful to look on "threshold" as a continuous variable T, with

$$T=1.66 \log (R/R_0) \tag{1}$$

where

$$R_0=0.25 \text{ mm hr}^{-1}=0.01016 \text{ in hr}^{-1}.$$

The right-hand ordinate scale of figure 1 is of $p(>R)$, the probability at any instant (within the season) of rainfall rate at the gage in excess of R (as specified by the abscissa). Taking $D(>R)$ to denote duration with rate in excess of R and θ to denote the total duration or length of the season, one obtains

$$p(>R)=D(>R)/\theta. \tag{2}$$

In place of a rain gage, there are two ways in which the distribution of $p(>R)$ with R can be obtained from a season's set of radar maps. Either way presumes a relation between the value of Z averaged over a volume aloft and the value of R at a point on the ground. One way is to accumulate data over the season for one point on the map. A more powerful alternative, if one can assume $p(>R)$ to have the same distribution with R at every point, is to use data from all over the map, or at any rate from a considerable prescribed area. In return for accepting an average distribution for an area in place of true statistics for a point, one obtains many times as many data in a single season.

Let an area B be mapped M times, at intervals Δt throughout the season, so that $M\Delta t=\theta$. Then, denoting the area with rainfall rate $>R$ on the M maps by $E(>R)$, one obtains

$$p(>R)=E(>R)/MB. \tag{3}$$

This would apply for any M maps that were representative of the season, if M were large enough, and the maps were either uniformly or randomly distributed throughout the season, so that times of maps were not correlated with times of precipitation. When we specify uniform intervals Δt, so that $M\Delta t=\theta$, we have

$$p(>R)=E\Delta t/\theta B. \tag{4}$$

The product $E\Delta t$ is (area$\times$duration) and will be expressed in n.mi.^{2} hr. It is a convenient measure of the extent, in area and time, of rain of rate $>R$, and a natural extension of the concept of $D(>R)$ for a point.

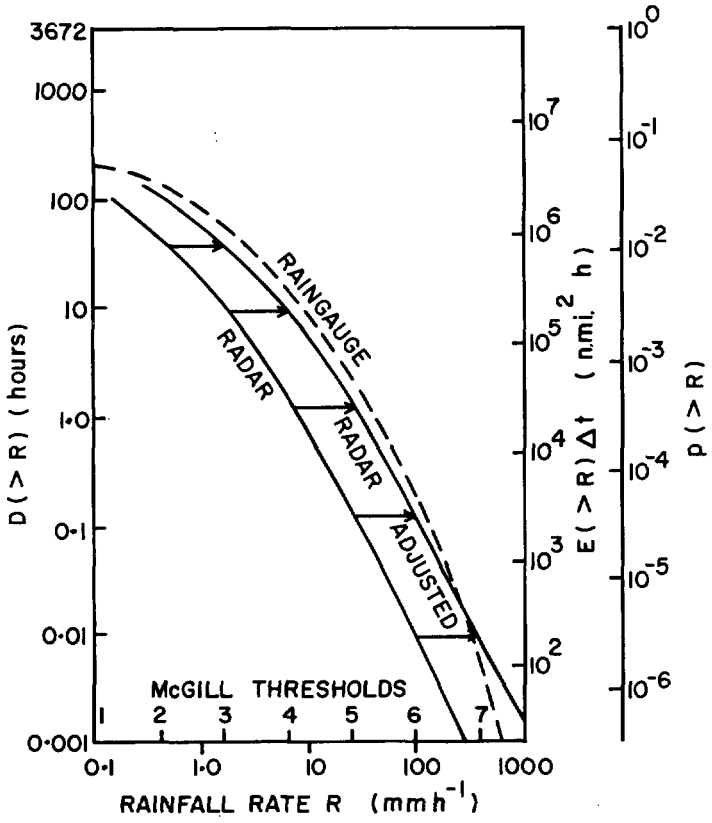

FIGURE 2.—Duration D and probability p at any point, also extent in map area times time, $E\Delta t$, of rain of intensity in excess of that given by the abscissa. "RADAR ADJUSTED" has been fitted to "RAINGAUGE" by moving "RADAR" to the right by one unit of "threshold." The need for this adjustment is attributed to attenuation of microwaves by rain.

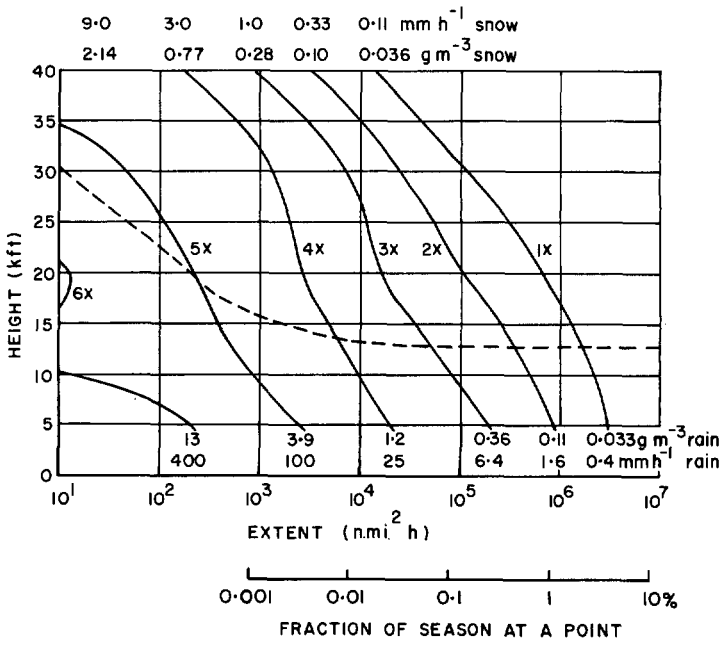

FIGURE 3.—Extent in map area times time of precipitation of intensity in excess of values indicated, for rain at the lower ends of the loci, for snow at the upper end. The values at height 5,000 ft have been fitted (approximately, as in fig. 2) to gage values at the surface. The broken line is the estimated boundary between rain and snow (or other precipitation made of ice with a dry surface).

In figure 2, $p(>R)$ has been obtained by radar at 5,000 ft with $B=20{,}000$ n.mi.^{2} (between ranges 20 and 80 n.mi. approximately) as well as by gage at the surface. While the radar data could have been obtained by planimetry on maps, in line with the foregoing paragraph, it was actually obtained by a device involving an oscillograph and camera, devised and used by Hamilton (1966). If the rain gage is representative of the radar region, and if the statistics for R are the same at 5,000 ft as at the surface, the gage and radar curves should be the same. There are several likely causes for the difference between the two curves. The cause of which we are most aware is the attenuation of microwaves by rain, which is considerable at wavelength 3.2 cm. Hamilton (1966) was the first to correct radar records for attenuation, etc., by a correction function obtained by bringing two such curves together. For the longer range of intensities considered here, we propose the simplest possible correction function, multiplying all rainfall rates obtained from radar by a factor 4. This adjustment is achieved by adding unity to each threshold (T) on the radar records and gives the radar data at 5,000 ft approximately the same statistics as gage data at the ground, which is reasonable.

3. PRECIPITATION STATISTICS ALOFT

Figure 3 gives the radar data for all heights for a summer season of 3,672 hr. The lines are labeled 1X, 2X, 3X, 4X, 5X, 6X, to indicate observations of thresholds 1 to 6, with X-band radar, without allowance for attenuation. The preceding section suggests that, at 5,000 ft, thresholds 1X, 2X, 3X, 4X, 5X, 6X be equated to McGill-1960 thresholds 2, 3, 4, 5, 6, 7 to allow for attenuation, etc. Interpretation of these thresholds at all heights is discussed in the following paragraphs.

Radar observes target strength in the beam and so relates to rain per unit volume, whereas rainfall rate is a flux. The assignment of a rate-of-rainfall value to a radar threshold implies either that the vertical motion of the air is negligible in comparison with the fall speed of the raindrops, or that the flux of rain is taken relative to the air, that is, to an imaginary gage rising or falling with the air. Updrafts and downdrafts greater than 1 m sec^{-1}, and so comparable with raindrop fall speeds, are only (or usually at any rate) found associated with cumulus clouds, and so with the higher rainfall rates (say 10 mm hr^{-1} or more). Because of the uncertainty associated with these vertical air motions and so with these higher rainfall rates, there is advantage in using rainfall density (or rainwater content, usually in gm m^{-3}) rather than rainfall rate. The importance of rainfall density is in describing the three-dimensional pattern of precipitation aloft; it is not relevant directly to the basic

TABLE 1.—*Thresholds and rain parameters*

Threshold:						
As observed	1X	2X	3X	4X	5X	6X
As interpreted for rain	2	3	4	5	6	7
Rain rate mm hr^{-1}	0.4	1.6	6.3	25	100	400
Rain density gm m^{-3}	0.033	0.11	0.36	1.2	3.9	13

TABLE 2.—*Thresholds and snow parameters*

Threshold	1X	2X	3X	4X	5X	6X
Snow rate mm of water hr^{-1}	0.11	0.33	1.0	3.0	9.0	
Snow density gm m^{-3}	0.036	0.10	0.28	0.77	2.14	

hydrological problem of amount of rainfall arriving at the ground. Table 1 relates the McGill-1960 thresholds, as observed at X-band and as interpreted, to rainfall rates and density, the latter reached by the relation $M=72\ R^{0.88}$.

Rate of snowfall is affected also by vertical air motions. The fall speed (about 1 m sec^{-1}) is less than for rain, and so generally are the associated vertical motions. Thus, for snow as for rain, precipitation density is a more convenient parameter (except for hydrology) than precipitation rate. In showers, snow is found in the low-density outer portions. It is not found in the intense cores where the vigorous vertical motions are, because there the hydrometeors, whether liquid or solid, grow by accretion in the dense cloud, and snow crystals are replaced by hydrometeors growing more in the manner of hail.

Attenuation is much less for dry snow and dry hail than for rain, and at X-band it can be neglected. Table 2 relates the thresholds, which do not need correction for attenuation, and so are not corrected at all to rate of snowfall in millimeters of liquid water per hour and snow density in gm m^{-3} (using $Z=2000\ R^{2.0}$ and $M=250\ R^{0.90}$ from Gunn and Marshall 1958). The density values for a given observed threshold are nearly the same for snow and rain at 1X and 2X, considerably greater for rain at 3X and 4X, almost twice as great for rain at 5X. A signal at threshold 6X is not likely to come from snow, but rather from some sort of hail, with a considerable chance of its surface being at an enhanced temperature and so wet.

The precipitation rate for snow increases more gradually with threshold than that for rain. Density, which we have noted is within 10 percent (of the density of rain of the same threshold) for light snow and within a factor 2 for heavy snow, is the parameter that can be considered without necessarily taking vertical motion of the air into account. So the isopleths of figure 3 (that is, 1X, 2X, etc.) can best be read in terms of precipitation density. Within a factor 2, which is not much when the problem of attenuation is borne in mind, the density values for rain can be accepted without change for snow, over its narrower range. A broken line has been drawn intuitively on figure 3 to indicate roughly the boundary between water and wet ice on the one hand and dry snow and dry ice generally on the other.

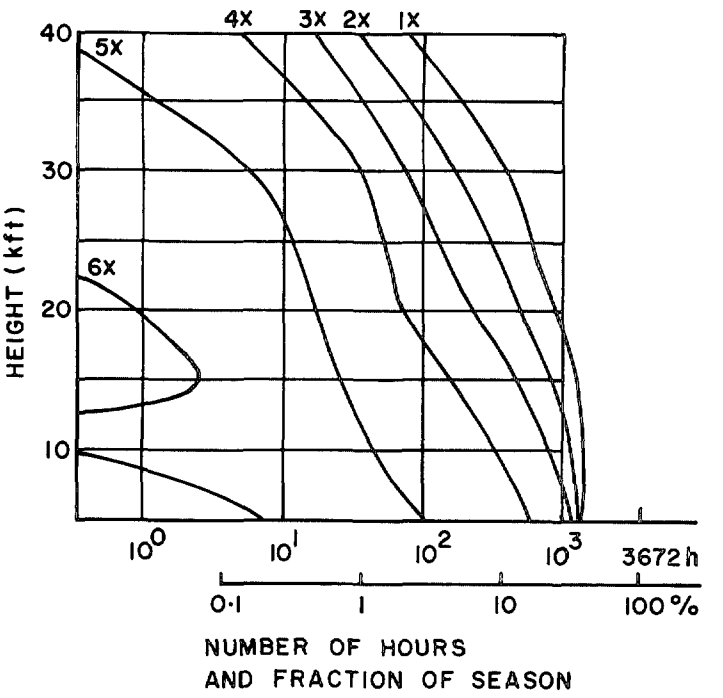

FIGURE 4.—Duration and probability that somewhere in the 20,000 n.mi.^{2} under surveillance there is precipitation of intensity in excess of the threshold values indicated on the loci.

The probability of precipitation somewhere in the 20,000 n.mi.^{2} under surveillance is much greater than the probability at a specified point (fig. 4). At the surface, it ranges from about 30 percent for thresholds 1X, 2X, and 3X to less than 0.2 percent (=7 hr) for *T*6X. The close spacing of lines 1X, 2X, and 3X below 15,000 ft suggests that on almost every shower map there is at least one shower that achieves some threshold 3X, and reaches heights above 15,000 ft. Decreasing the sensitivity of the radar by 20 dB (from 1X to 3X) would decrease the hours when showers were detected somewhere (at height 5,000 or 10,000 ft) only a few parts percent. At the same time, the area of target revealed would be decreased by a factor 10, to judge by figure 3.

4. SEPARATE TREATMENT OF TALL-STORM MAPS

There is much evidence that the chance of a shower revealing severe-storm characteristics increases with its height. In figure 5, the statistics for 75-hr maps, each containing one or more storms that reach 40,000 ft (solid curves), have been separated out from the rest (broken curves). For the tall-storm maps, the extent in space and time remains constant or increases slightly with height to about 20,000 ft; the rate of decrease with height above 25,000 ft is still much less than for the broken lines. At 5,000 ft, the tall-storm maps account for a small fraction

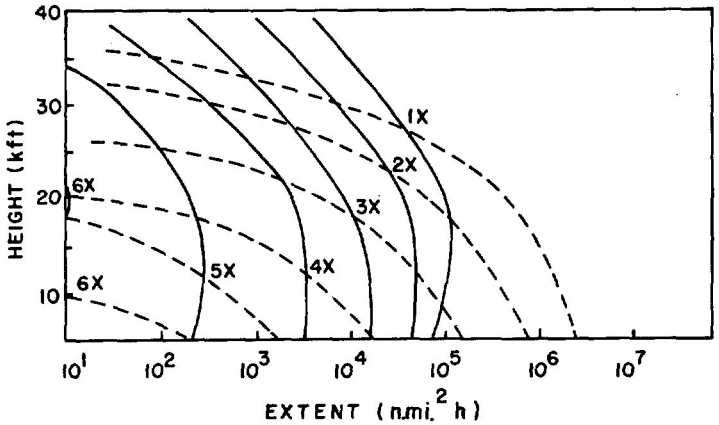

FIGURE 5.—Extent in map area times time of precipitation with intensity in excess of the threshold values indicated on the loci. The solid lines are for times when some precipitation extended to height 40,000 ft. The broken lines are for all other times.

of the extent for the season. At 20,000 ft, the tall-storm maps still make only a minor contribution at thresholds less than 3X, but they contribute the major part at thresholds 4X and 5X.

5. PATCHES AND THEIR DISTRIBUTION WITH SIZE

At the same time that the foregoing data were being recorded by Hamilton's integrating device, actual constant-altitude maps (CAPPI) were being made, one set of maps for six altitudes every 22½ min.

The pattern on the maps (fig. 6) could generally be analyzed in terms of showers or cells with central maxima. Before proceeding with such analysis, a word about the absence of detail is in order. These maps first appeared on a cathode-ray tube, and the size of the spot formed on the phosphor by the electron beam limited the resolution. The tube face was photographed, and the photographs were scanned by a flying spot scanner, working slowly in a rectangular raster, and feeding a facsimile receiver. Again, the size of the spot limited the resolution, and this time the spot was large enough, intentionally, to give considerable areal integration and so reduce the random-phase fluctuations that are inherent in radar-weather records. The sharp boundaries appearing in figure 6 are the result of electrical thresholds applied to the output of the flying spot scanner, after all that areal integration. The integration made the boundary lines smoother than they would have been otherwise, and removed much detail that existed in the actual precipitation pattern. To judge by rain-gage records, the actual pattern contained steep gradients that could perhaps be described best as discontinuities in R; this sort of detail is lost in the present maps. In the future, it should be possible to have improved systems that reduce random-phase fluctuations adequately while leaving much more detail. In considering the present analysis, the removal of detail and of steep gradients should be borne in mind.

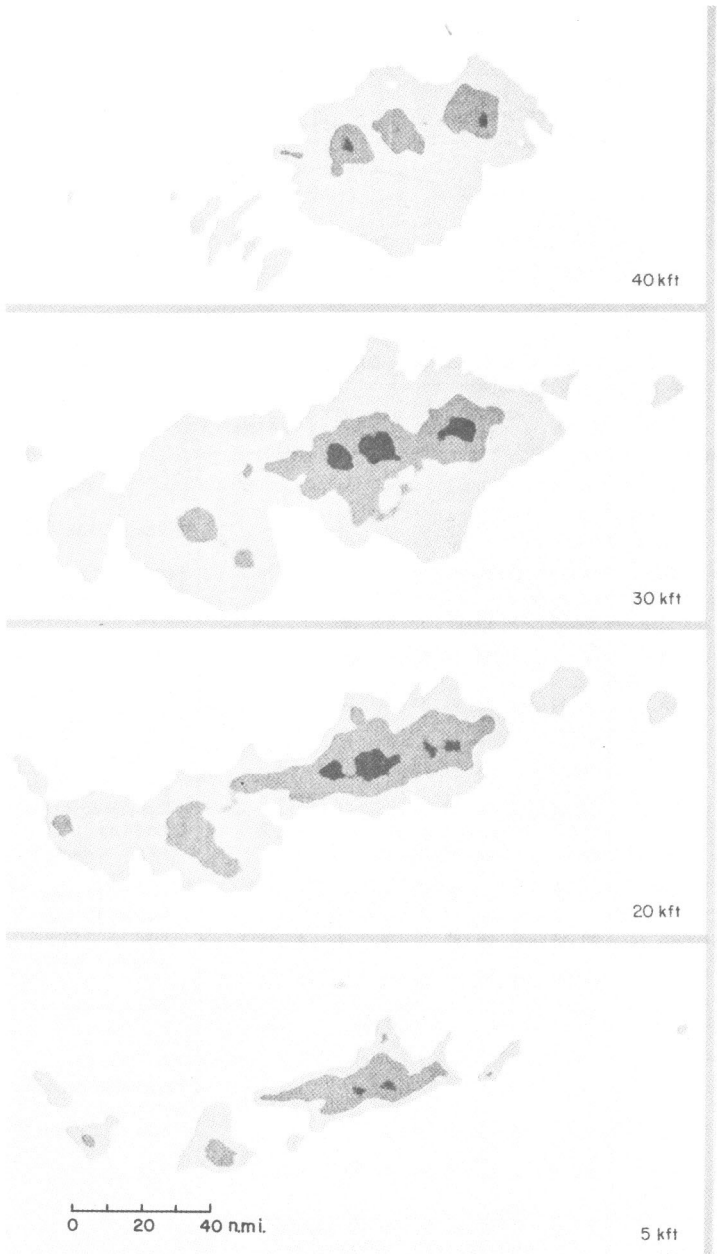

FIGURE 6.—Storm of July 18, 1964, studied intensively by Holtz (1968), mapped in constant-altitude sections. Boundaries appear at thresholds $T1X$, $T3X$, $T5X$, and a companion set not shown gives the intermediate thresholds.

Figure 6 shows a group of showers or cells. Thresholds appear as boundaries between discrete shades of gray. The shade bounded on the outside by Tn is called shade n. The whole of the region bounded by Tn is called a Tn patch. It is liable to contain a $T(n+1)$ patch, which may in turn contain a $T(n+2)$ patch, and so forth (fig. 7).

The actual analysis was done in terms of the patches within the various thresholds, and their distribution with size. The arraying of patches, one within the other, to form cells or showers was considered afterward, on the basis of the patch statistics, and neglecting cases

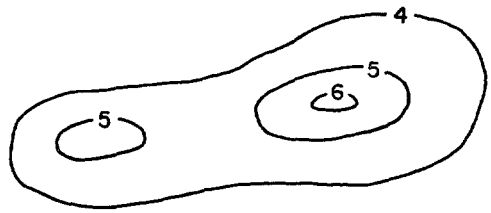

FIGURE 7.—Situation described as one $T4$ patch containing two $T5$ patches, one of which contains a $T6$ patch.

TABLE 3.—*Distribution with area of a number of patches*

Height (kft)*	Area in square (statute) miles 1	2	4	8	16	32	64	128	256	512	1024	
40	2	2	7	19	10	3	6	3				
30	4	1	18	37	31	16	4	6	5		1	Threshold 4 patches
20	8	9	19	39	41	24	15	11	7	4	1	Data from:
15	13	8	23	60	39	30	20	12	4	4	1	July 2, 8 maps
10	9	10	25	35	55	34	32	17	6	3	1	Aug. 30, 10 maps
5	8	12	34	51	65	31	27	13	13	2	2	
40	1	4	4	1	6	2						
30	5	15	12	19	10	10	5					Threshold 6 patches
20	18	19	29	29	20	23	12	1				Data from:
15	49	31	55	65	37	27	10	3	1			July 2, 8 maps
10	59	66	81	79	65	31	23	5	3	1		July 18, 17 maps
5	48	58	100	93	82	57	19	22	4	2	1	July 29, 11 maps
												Aug. 15, 22 maps
												Aug. 30, 8 maps
20	2	1		1								
15	3	1	4	5	5	1	1					Threshold 7 patches
10	6	4	11	11	2	4	1					Data from:
5	29	17	28	31	13	10	8	3	1			Aug. 15, 25 maps
(kft)* Height	1	2	4	8	16	32	64	128	256	512	1024	
	Area in square (statute) miles											

*(kft) = thousands of feet.

TABLE 4.—*Distribution with area of threshold 6 patches with and without threshold 7 patches*

Height (kft)	Area in square (statute) miles 1	2	4	8	16	32	64	128	256	512	1024	
20	8	3	3	1	0	0	0	0	0	0	0	
	1	1	0	0	0	1	1	0	0	0	0	
15	14	11	11	9	2	0	0	0	0	0	0	Threshold 6 patches
	0	0	2	2	3	1	2	0	1	0	0	Without 7 (upper number)
10	34	39	39	18	6	2	1	0	0	0	0	With 7 (lower number)
	0	0	2	6	9	4	3	1	2	0	0	
5	33	31	53	48	26	11	0	0	0	0	0	
	0	0	3	11	19	18	11	16	3	2	1	

TABLE 5.—*Distribution with area of threshold 4 patches with and without contained threshold 6 patches*

Height (kft)	Area in square (statute) miles 1	2	4	8	16	32	64	128	256	512	1024	
40	1	2	7	18	10	2	6	2	0	0	0	
	0	0	0	1	0	1	0	1	0	0	0	
30	4	1	18	36	31	15	4	1	0	0	0	
	0	0	0	1	0	1	0	5	5	0	1	
20	8	9	19	39	40	24	13	6	1	1	0	Threshold 4 patches
	0	0	0	0	1	0	2	5	6	3	1	Without 6 (upper number)
15	13	8	23	60	38	26	13	6	0	2	0	With 6 (lower number)
	0	0	0	0	1	4	7	6	4	2	1	
10	8	10	25	35	54	31	21	8	1	1	0	
	0	0	0	0	1	3	11	9	5	2	1	
5	8	12	34	51	60	29	20	4	2	0	0	
	0	0	0	0	5	2	7	9	11	2	2	

where one Tn patch contained more than one $T(n+1)$ patch, as for example the $T4$ patch in figure 7 which contains two $T5$ patches.

For this work on patches and showers, we have used thresholds 2, 3, 4, 5, 6, 7 to denote observed thresholds 1X, 2X, 3X, 4X, 5X, 6X, which is correct for rain (table 1) and approximately correct, *as regards density*, for snow (table 2).

The census of patches was limited to $T4$, $T6$, and $T7$ patches, on selected sequences of maps. A condition for selection was that the sequence should contain a threshold 6 at some height, at some time in the sequence. The census yielded the distribution of the number of patches with patch-area A of table 3. The table shows a decrease in numbers with height, but analysis did not reveal any significant change in the size distribution with height.

One can predict the size of a growing Tn patch at which an $(n+1)$ threshold or an $(n+2)$ threshold will appear within it. (This predictability might be exploited operationally, estimating core intensity from area within a contour of relatively low intensity.) In table 4, observe that patches of area greater than 64 mi^2 almost always contain a higher threshold, and those of area less than 8 mi^2 hardly ever do. In table 5, patches of area greater than 256 mi^2 almost always contain *two* higher thresholds, while those of area less than 16 mi^2 hardly ever do. Thus, there is a transitional range of sizes, below which a patch never contains a higher threshold, above which it always does.

The census having been conducted on sample sequences, there was a need to adjust the data so that it represented a whole summer. The number of maps M has been adjusted to 5,000, each of area B=20,000 n.mi.^{2}, so that the total number of square miles MB comes to the round number 10^8. Figure 8, obtained on this basis, gives for thresholds 4, 5 (by interpolation), 6, and 7 the numbers of patches N of area greater than A, for 5,000 maps each

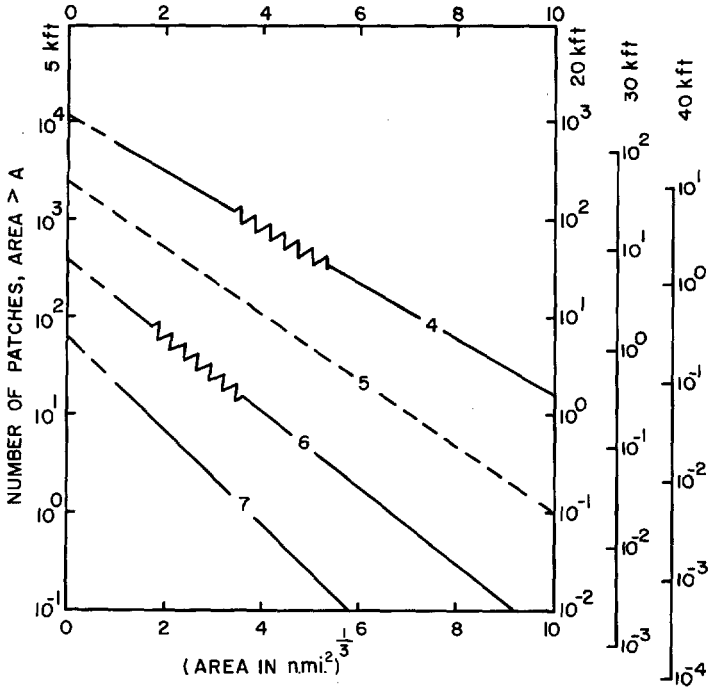

FIGURE 8.—For $MB=10^8$ n.mi.², numbers of $T4$ patches, $T5$ patches, etc. of area greater than indicated by the abscissa, with ordinate scales for four different heights. We picture $MB=10^8$ as made up of a number of maps $M=5{,}000$, for hourly maps through a season of 5,000 hr, and $B=20{,}000$ n.mi.² as the area of an individual map. The locus for $T5$ was interpolated. On the $T4$ locus, patches in the zigzagged section might or might not contain $T6$ patches. On the $T6$ locus, patches in the zigzagged section might or might not contain $T7$ patches.

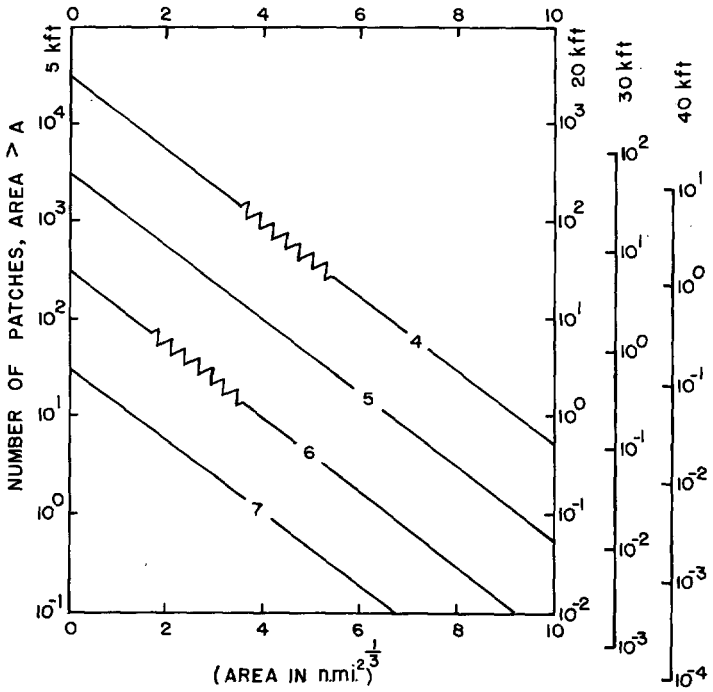

FIGURE 9.—For $MB=10^8$ n.mi.², numbers of patches of area greater than indicated by the abscissa for various heights. Small adjustments have been made to the loci of figure 8 such that they now all have the same slope.

of area 20,000 n.mi.², or total area 10^8 n.mi.² Regarding the abscissa in figure 8, we recall that in the tables a logarithmic scale of area was used, but it was found that log-log plots of number against area were not very helpful. Log number against square root of area showed some promise, but the locus was not linear. Log number against cube root of area approximated well to straight lines.

After having first found straight lines for the pooled data from all heights, it was possible to go back and confirm the validity of the same relation at single heights for fewer data. Thus the same lines on the figure will serve for all heights, provided separate scales are used for various heights. The variation with height of total area within any threshold is such (for thresholds 4 to 7, at any rate) that to a usable approximation the variation of scale with height can be kept very simple.

The zigzagged sections of the loci in figure 8 represent the transitional regions already mentioned. On the $T4$ line, patches to the left of the zigzagged section never contain a $T6$, while those to the right of that section always contain a $T6$. On the $T6$ line, patches to the left of the zigzagged section never contain a $T7$, and those to the right always do.

For any one of the loci of figure 8, there is a relationship between the total area, the slope of the locus, and the intercept N_0 with the axis of log number. In figure 9, a common slope has been introduced as a helpful further approximation, while maintaining the correct relation between total area, slope, and intercept. The equation of the loci of figure 9, relating number of patches to patch size within a given threshold, is

$$\log N=\log N_0-x=8.8-T-H-x$$

or

$$N=N_0e^{-2.3x}=e^{2.3}(8.8-T-H-x) \qquad (5)$$

where x is the size parameter, related to the area A within the given threshold by

$$x=A^{1/3}/2.6 \text{ n.mi.}^{2/3}=(A/17.5 \text{ n.mi.}^2)^{1/3}. \qquad (6)$$

N is the number of patches at any instant, at height H of size greater than x, per 10^8 n.mi.² of map area, as for 5,000 maps each of area 20,000 n.mi.², or alternatively N is the number of patches times time, during a 5,000-hr season of surveying 20,000 n.mi.²; H is height/(15,000 ft); and N_0 is the value of N when $x=0$, so

$$\log N_0=8.8-T-H. \qquad (7)$$

The analysis supports these relations only for $T=4, 5, 6, 7$; and for $T=7$, the variation with height is not supported. More generally, the variation with height applies to statistics for a whole season. It should apply approximately on individual days, except on days when some storms

reach 40,000 ft (fig. 5), and it is not relevant to individual storms.

6. MODEL HORIZONTAL SECTION THROUGH A CELL

In figure 9, picture one horizontal line for each integer on the ordinate scale, so that there are 90 lines between 10^1 and 10^2, for example. Each such line can represent a horizontal or map section through a cell, specifying by its intersections with the sloping loci the sizes of a set of patches, one within the other. This assumes that (for example) the $T5$ patches in order of their size fall within $T4$ patches taken in the same order. This seems to be approximately correct, if we neglect cases of two $T5$ patches within one $T4$ patch (for example).

Each horizontal section through a cell, which would be denoted by a horizontal line in figure 9, has a maximum value of T at the center or core, which we shall denote by T_c, from which T decreases with increasing area, linearly with increasing x. The values of N and T for $x=0$ are interrelated:

$$\log N_0 = 8.8 - T_c - H \qquad (8)$$

where N_0 is the number of cells with central maximum (in horizontal section at the specified height) in excess of T_c. For a convenient example, we might take $H=1.8$ (for height=27,000 ft) and find, for the conventionalized season, one patch reaching maximum intensity in excess of $T7$, 10 patches in excess of $T6$, 100 in excess of $T5$, etc.

For any cell (in horizontal section), the value of T bounding area A is given by

$$T = T_c - x \qquad (9)$$

where x is given by equation (6). Thus, the values of parameters R, M, and Z bounding area A decay exponentially with x. Introducing equation (1), we obtain, for example, for the value of rainfall rate bounding area A:

$$R = R_c e^{-1.38x}. \qquad (10)$$

Equations (9) and (10) apply to idealized cells. Equation (8) gives the number of such cells; without depending on the idealization, it gives the number of cores with central intensity in excess of any given value (specified in terms of threshold).

7. SHAPE OF PATCHES AND CELLS IN HORIZONTAL SECTION

For each of 140 patches of various areas A and at various heights, a best fitting rectangle was taken, of the same area as the patch, with minimum extent a and maximum extent b, so that $ab=A$. In figure 10, A has been plotted against a, and envelopes and a median locus have been drawn. The lower envelope has $a=b=A^{1/2}$; it is predetermined when by definition a is made not greater than b. For the upper envelope, $b=6a$. Thus the largest and smallest extents are always within a factor 6 of each other, and so within a factor 2.45 of $A^{1/2}$. The locus $b=2a$, paralleling the two envelopes, divides the data into approximately equal groups on either side, so that 2 is a median value for the aspect ratio b/a.

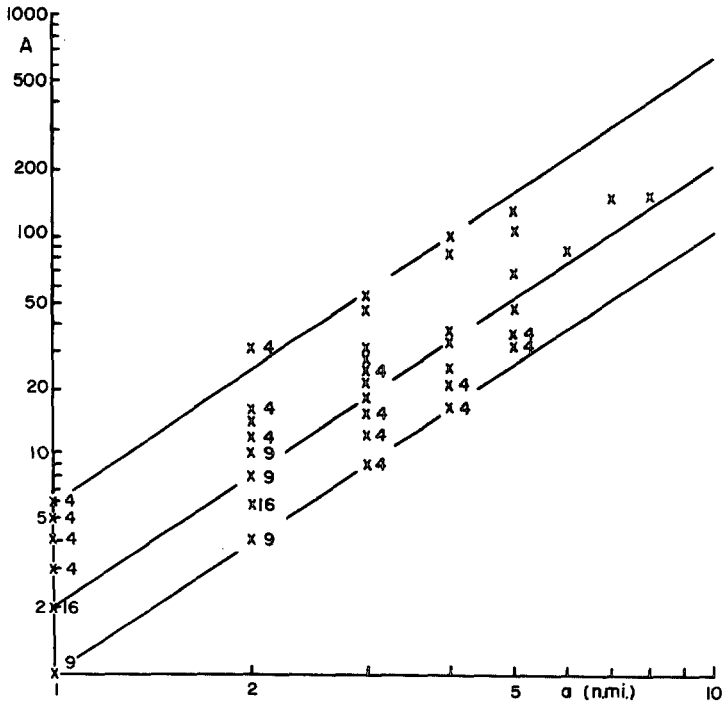

FIGURE 10.—Area A of the patch and of the best fitting rectangle plotted against the smaller side a of the rectangle. A cross with a number beside it stands for that number of data. The middle line is for the median value of A; for a given value of a, the top and bottom lines have been drawn as envelopes to contain very nearly all the data.

Figure 11 shows model cells with the median shape $b=2a$, with numbers to be expected in hourly maps for one summer at height 27,000 ft, the example given in the preceding section: one cell with $T_c=7$, 10 with $T_c=6$, 100 with $T_c=5$. The relationship between area and threshold that we have used has only been tested down to $T=4$. Patterns with $T_c=4$, 3, 2 are doubly extrapolated, and progressively less reliable.

For three reasons, figure 11 must not be taken to indicate gradients: 1) the data do not give evidence of the symmetry that has been introduced into the diagrams for simplicity, 2) the resolution of the radar and display as used were not sufficient to reveal details and extreme gradients that are indicated by some rain-gage records, and 3) distortion by attenuation makes the details unreliable—attenuation introduces a negative term into the gradient (with range) which in intense rain may exceed the gradients we have observed.

8. INTEGRATED AMOUNT OF RAIN WATER

For a horizontal *layer* or storm of vertical extent Δz, the mass of rainwater can be calculated either from the model

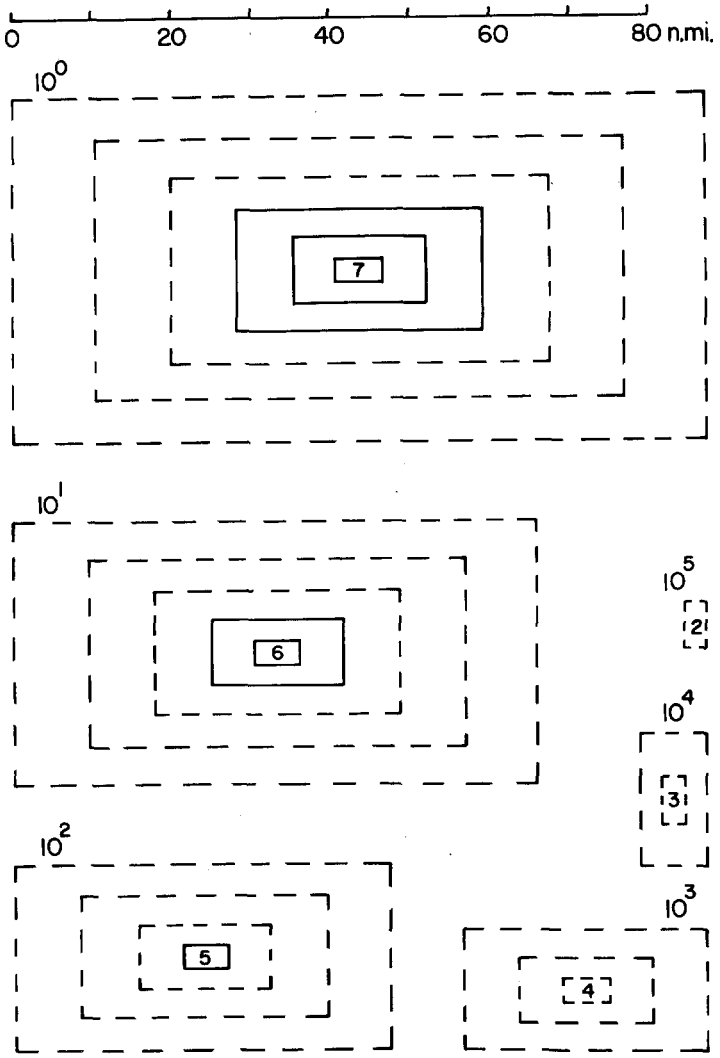

FIGURE 11.—Using median shape for cells, contours or threshold lines have been drawn against a common scale of distance, for T_c=7, 6, 5, etc. The number of cells larger (and with larger T_c) than the cell shown appears at the top left of each diagram. Everything outside $T4$ is extrapolated.

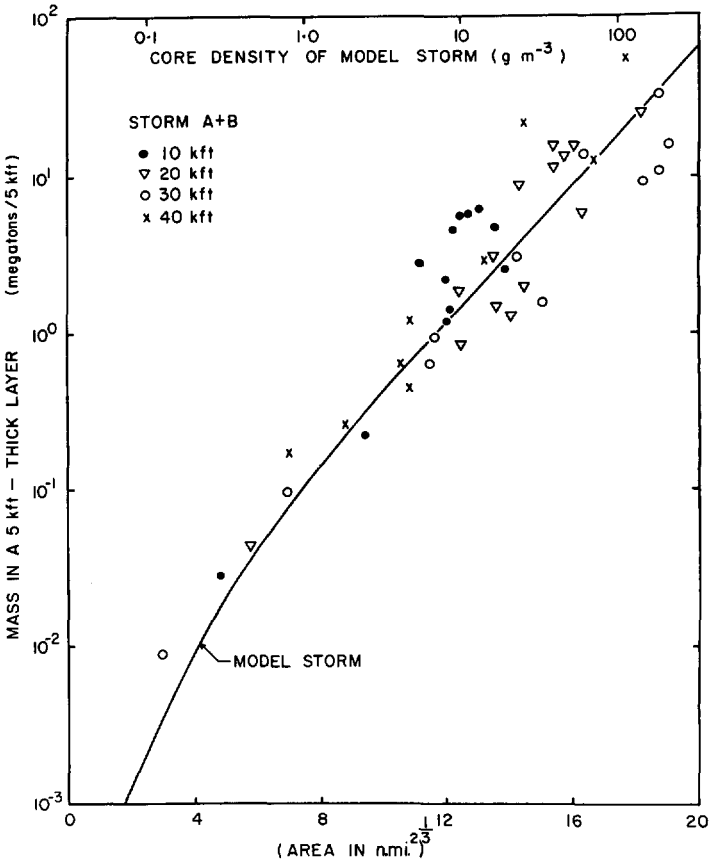

FIGURE 12.—Mass of a 5,000-ft-thick layer of a cell, plotted against an area in the horizontal section within $T2$. The data points are based on radar observations of "storm $A+B$" of July 18, 1964; the locus is based on the idealized cell.

cell or from the horizontal section given by a CAPPI map. In figure 12, the data points give area within $T2$ (abscissa) and mass in a 5,000-ft layer (ordinate), the latter calculated from the areas within the various thresholds for the storm of July 18, 1964, studied by Holtz (1968), for which sample maps appear in figure 6. For the curve, the mass was calculated from the area within $T2$, using the model cell. The observed masses (data points), based on the structure as revealed by radar, fall within a factor 3 of the mass given by the curve, for which radar provided only the area within $T2$, and the model provided the structure, that is the areas within other thresholds. Note that the curve approaches a straight line, by which the mass increases exponentially with x, and that most of the data fall on this practically straight section of the curve, and the rest fall just as well on the straight section extrapolated.

Significantly, the same curve fits the data from all heights equally well. Thus for the July 18 storm, the model horizontal section applies without adjustment at any altitude. For this storm, which was not the basis of the relationship, the total mass of precipitation in the storm and the distribution of mass with height could be determined from measurements of the horizontal area of the storm as a function of height.

9. OVERHANGING PRECIPITATION AREAS

Figure 3 shows the total extent of precipitation (in n.mi.^{2} hr) to drop off with height; figure 5 makes an exception of the tall storms, for which the total extent tends to be slightly greater at 20,000 ft than at 5,000 ft; and figure 6 shows an example of the tall-storm class. In the study of horizontal sections, no attention was paid to the variation of area with height in individual showers. A brief search was made, however, for "overhangs." The overhang was taken as the excess of the horizontal area within a given threshold at 20,000 ft over that for the same shower at 5,000 ft.

For the months of July and August 1963, overhangs were found in 17 percent of the map sets (excluding those

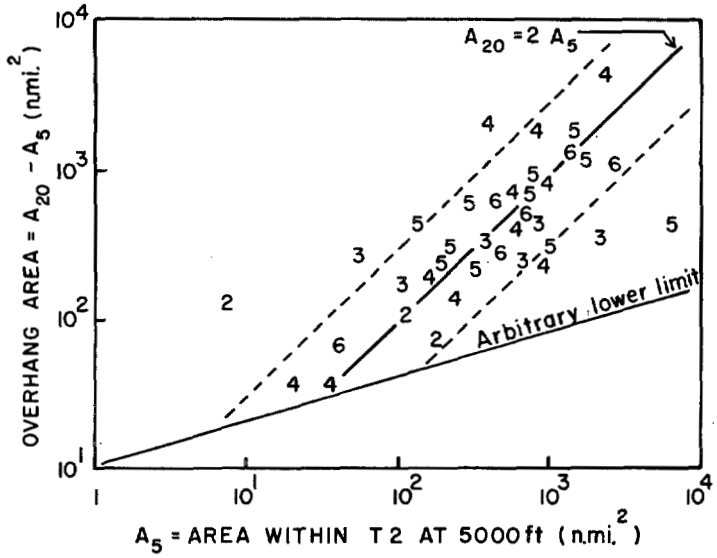

FIGURE 13.—Overhang (area within $T2$ at 20,000 ft minus the area at 5,000 ft) plotted against an area at 5,000 ft. The digits used in place of points in plotting these data give by their values the largest value of T for which an overhang is recognizable. The solid-line locus is for an area at 20,000 ft double the area at 5,000 ft.

sets where the precipitation was all below 20,000 ft). But in these 33 map sets with overhangs, there were only 37 overhangs (at $T2$), and many times that many patches. When the threshold was advanced from 2 to 3, 4, 5, and 6, the number of overhangs dropped from 37 to 34, 28, 17, and 6. Figure 13 shows the overhangs at $T2$. Each is marked by the greatest value of threshold at which it was recognizable as an overhang. The locus that appears as a good fit to the data is for overhang area equal to base area, that is an area at 20,000 ft twice the area at 5,000 ft. Ten percent of the overhangs have less than one-third the base area, and 10 percent are more than three times as large. An arbitrary lower limit is shown; overhangs smaller than this were neglected. These cases of overhang would in general be identifiable with the tall-storm situations already mentioned: for situations in which storms reached 40,000 ft, the area within any threshold, totaled over all cells, tends to increase slightly with height to maxima at about 20,000 ft. Apparently, then the usual thing is for cells (considered in three dimensions) to decrease in horizontal area (within any boundary value of T) with increasing height, but cells of heights that are exceptional for the whole season are liable to have a maximum horizontal extent at about 20,000 ft. At $T2$, this maximum extent may be anything up to four times the extent at height 5,000 ft. Apart from these exceptional cases, cells decrease in area (within any boundary value of T) with increasing height.

10. SUMMARY

The distribution of rainfall duration with rainfall rate, for a point on the earth's surface (McGill Observatory), for one summer season, was derived from the data of a recording rain gage. A new ordinate scale converts this to probability distribution. (Conversion from duration to amount of rainfall would be straightforward. Conversion of the abscissas from rate of rainfall R to any function related to R, such as rainwater content M or the radar reflectivity parameter Z, would be simple.)

From weather radar records, the distribution of rainfall extent in map area and time was obtained for the same season for every height from 5,000 to 40,000 ft. This extent in area and time (n.mi.^{2} hr) can be divided by the area under surveillance to give the distribution of duration at a point, if it is assumed that all points in the area under surveillance have the same distribution. Conversely, of course, the duration distribution from the rain gage can be converted to extent in area and time, on the same assumption.

The radar distributions for all heights were adjusted, without change in shape, so that the radar distribution for 5,000 ft fitted the gage distribution at the surface. This provided a statistical calibration of the radar by the gage, compensating in a way for the attenuation by rain suffered at the 3.2-cm wavelength that was used.

The principal variation with height that was found was a decrease of extent and duration by a factor 10 for every 15,000-ft increase in height, from 5,000 to 40,000 ft.

The precipitation pattern in constant-altitude sections was analyzed in terms of cells. At any height, the number N_0 of cells with maximum intensity in excess of a given value of T_c was found to be given by $\log N_0 = 8.8 - T_c - H$ (equation 8), where H is height/(15,000 ft),and T_c like any other value of T is related to R (for example) by equation (1). Within each cell, the value of T bounding area A containing the point of maximum T is given by $T = T_c - x$ (equation 9), where $x = (A/17.5 \text{ n.mi.}^2)^{1/3}$. The findings of this analysis by cells contains the previously described findings regarding distribution, with R and variation with height somewhat simplified.

The information about cell structure provided by equation (9) and in less conventionalized form by tables 4 and 5 appear relevant to current operational problems in the prediction of severe-weather events. Specifically, area within any given constant-intensity contour is an indicator of peak intensity and of area within any other constant-intensity contour. The area within a contour at about $R = 10$ mm hr^{-1} might be obtainable more reliably, particularly at attenuating wavelengths, than areas within higher intensity contours or peak intensity.

Shapes of cells were studied to the limited extent of the length and width of the best fitting rectangle of the same area as the cell for any bounding value of T. The ratio of length to width (taking length as the larger) was most likely to be unity. It had a half chance of being less than 2:1, and was always less than 6:1.

While this analysis was in terms of cells in the constant-altitude precipitation pattern, only a small study was made of the cells as three-dimensional entities. For the central part of the season (July and August), one map set

in six had cases of "overhang"—cells that increased in size with increasing height, specifically that were larger at height 20,000 ft than at height 5,000 ft. Of the many cells on one map, there was seldom more than one with overhang. These cases of overhang at about 20,000 ft would in general be identifiable with the tall storms that reached 40,000 ft.

We recognize two weaknesses in the input data to this study: 1) the radar utilized wavelength 3.2 cm, for which attenuation is considerable, and our correction for this was rudimentary, and 2) areal integration in the display system reduced resolution and removed high gradients or discontinuities. The present study should be replaced by one without these limitations, and studies of the same general sort in a variety of climates are needed.

ACKNOWLEDGMENTS

The records that have been analyzed were obtained from the McGill Weather Radar, the operation of which, for research purposes, is supported by a grant from the National Research Council of Canada. Publication of this paper is with the permission (apropos the participation of Dr. Holtz) of the Director of the Canadian Meteorological Service.

REFERENCES

Altman, Frederick J., "Preliminary Correlations of Radar and Surface Climatologies," *Proceedings of the 13th Radar Meteorology Conference, McGill University, Montreal, August 20–23, 1968*, American Meteorological Society, Boston, **1968**, pp. 290–293.

Cataneo, R., "A Method for Estimating Rainfall Rate-Radar Reflectivity Relationships," *Journal of Applied Meteorology*, Vol. 8, No. 5, Oct. **1969**, pp. 815–819.

Gunn, K. L. S., and Marshall, J. S., "The Distribution With Size of Aggregate Snowflakes," *Journal of Meteorology*, Vol. 15, No. 5, Oct. **1958**, pp. 452–461.

Hamilton, P. M., "Vertical Profiles of Total Precipitation in Shower Situations," *Quarterly Journal of the Royal Meteorological Society*, Vol. 92, No. 393, July **1966**, pp. 346–362.

Holtz, C. D., "Life Cycle of a Summer Storm From Radar Records," Ph. D. thesis, McGill University, Montreal, **1968**, 141 pp.

Kessler, Edwin, "Computer Program for Calculating Average Lengths of Weather Radar Echoes and Pattern Bandedness," *Journal of the Atmospheric Sciences*, Vol. 23, No. 5, Sept. **1966**, pp. 569–574.

Kessler, Edwin, and Wilk, Kenneth E., "Radar Measurement of Precipitation for Hydrological Purposes," *WMO/IHD Project Report* No. 5, World Meteorological Organization, Geneva, **1968**, 46 pp.

Marshall, J. S., Holtz, Clifford D., and Weiss, Marianne, "Parameters for Airborne Weather Radar," *Scientific Report* No. MW–48, Stormy Weather Group, McGill University, Montreal, **1965**, 43 pp.

Marshall, J. S., Langille, R. C., and Palmer, W. McK., "Measurement of Rainfall by Radar," *Journal of Meteorology*, Vol. 4, No. 6, Dec. **1947**, pp. 186–192.

Rogers, R. R., and Rao, K. M., "Attentuation Statistics for Application to Microwave Communication Links," *Proceedings of the 13th Radar Meteorology Conference, McGill University, Montreal, August 20–23, 1968*, American Meteorological Society, Boston, **1968**, pp. 286–289.

Stout, Glenn E., and Mueller, Eugene A., "Survey of Relationships Between Rainfall Rate and Radar Reflectivity in the Measurement of Precipitation," *Journal of Applied Meteorology*, Vol. 7, No. 3, June **1968**, pp. 465–474.

Weiss, M., "The Distribution of Rainfall With Rate at McGill Observatory," M.S. thesis, McGill University, Montreal, **1964**, 113 pp.

[*Received September 15, 1969; revised December 8, 1969*]